

# Induced size effect on $\text{Ni}_x\text{Co}_{1-x}\text{Fe}_2\text{O}_4$ ( $0.1 \leq x \leq 0.9$ )

Ajay Shankar<sup>1,2,\*</sup>, Sandeep Kumar<sup>1</sup>, Sanjeev Thakur<sup>2</sup>, Rajni Porwal<sup>1</sup> and R. P. Pant<sup>1</sup>

<sup>1</sup>National Physical Laboratory, Dr. K.S. Krishnan Marg, New Delhi 110012, India

<sup>2</sup>Netaji Subhas Institute of Technology, University of Delhi, Sector-3, Dwarka, New Delhi 110078, India

\*Corresponding author. Tel: (+91) 11-4560-8309; E-mail: [ajayshankar0@gmail.com](mailto:ajayshankar0@gmail.com).

Received: 08 June 2012, Revised: 17 July 2012, Accepted: 18 July 2012

## ABSTRACT

Nanocrystalline  $\text{Ni}_x\text{Co}_{1-x}\text{Fe}_2\text{O}_4$  were synthesized and studied for their structural and magnetic properties. The effect of doping ion concentration on lattice parameter, crystallite size and the lattice strain pertaining to the ionic radii has been investigated. Electron microscopy supports the parameters and gives morphological view of the system. The magnetic measurement reveals the information on the effect of stoichiometry variation in existing superparamagnetism. Further, the spin dynamics and their role on dipolar interactions, extent of superexchange and spin-spin relaxation among nanoparticles have been investigated. Also, an attempt has been made to understand the UV irradiation effect on photosensitive  $\text{Co}^{2+}$  ion on Ni ferrite by in-situ electron spin resonance measurements. Copyright © 2012 VBRI Press.

**Keywords:** Core-shell structure; strain; superparamagnetism; ESR; dipolar interactions.



**A. Shankar** received his B.Sc. and M.Sc. in Chemistry from University of Delhi. Currently, he is working as a Senior Research Fellow at NPL (CSIR) and NSIT (University of Delhi). His field of research interest includes magnetic nanoparticles, ferrofluids and MR fluids and their applications.



**Sandeep Kumar** pursuing his Ph.D. from National Physical Laboratory (NPL), affiliated to Council of Scientific and Industrial Research (CSIR). His major research interests include synthesis of doped-ferrofluid and to study electron paramagnetic resonance (EPR) properties of different size nanoparticles which are well dispersed in different carrier liquid.



**R. P. Pant**, Senior Principal Scientist at CSIR- NPL, India obtained his PhD degree from Bhavnagar Univ. in 1993. His research interests include synthesis and characterization of nonmagnetic particles for ferrofluids applications. The characterization includes investigations of super paramagnetic particles, core shell structure, exchange bias interaction by ferromagnetic resonance techniques in low temperature.

## Introduction

During past few decades, nanomaterials have attracted researchers worldwide due to their unprecedented promising future applications while simultaneously involving basic and interdisciplinary sciences [1-5]. In this field, magnetic nanomaterials exhibit unique physical and chemical properties & have varieties of promising technological applications like ferrofluid, magnetic recording, color imaging, ceramics, catalysts and high frequency devices [6-10]. The size, shape, composition, and method of preparation strongly influence the magnetic properties of nanoparticles [11-17]. Ferrosinels ( $\text{AB}_2\text{O}_4$ ) exhibit magnetic properties, which mainly depend on the occupancy of interstitial sites by  $\text{A}^{2+}$  and  $\text{B}^{3+}$  in cubic close pack arrangement of oxide ions. In particular,  $\text{Co}^{2+}$  has been well studied for its significant effect on the magnetic properties of magnetite at nano level [18, 19]. Giri et al. [20, 21] reported the variations in coercivity of sol-gel synthesized  $\text{CoFe}_2\text{O}_4$  nanoparticles with change in particle size, temperature, and light intensity. On the other hand, Prussian blue ( $\text{M}_{1-2x}\text{Co}_{1+x}[\text{Fe}(\text{CN})_6]_z\text{H}_2\text{O}$ ; x and z are variables and M is an alkali metal) are very famous photomagnetic materials due to their non-stoichiometric composition, which in turn considered to be the cause for their photomagnetic effect [22]. The effect of annealing temperature on particle size, coercivity, strain, lattice parameter, saturation magnetization of nanocrystalline  $\text{CoFe}_2\text{O}_4$  has been discussed by V. Kumar et al. [23]. Silica coated  $\text{CoFe}_2\text{O}_4$  has also been recently used to tune some of its magnetic properties [24, 25]. Anomalous magnetic properties of nano  $\text{NiFe}_2\text{O}_4$  at low temperatures led Kodama et al. to propose ferrimagnetically aligned core

spins and a spin-glass-like surface layer [26-28]. Recently, nickel ferrite thin films have been investigated and their optical bands were found independent to the thickness of film [29]. The spin dynamics of these materials changes with temperature, magnetic phase transitions and photo-induced magnetic effect in various spinel ferrites has been investigated earlier [20, 21, 30-32]. So far, a little attention has been made to the tuning of photomagnetic property in cobalt ferrite via doping concentration of other cations. In the present work, we have explored the effect of mutual doping ion concentration of  $\text{Ni}^{2+}$  &  $\text{Co}^{2+}$  on structural and as well as magnetic characteristics of nanocrystalline  $\text{Ni}_x\text{Co}_{1-x}\text{Fe}_2\text{O}_4$  ( $0.1 \leq x \leq 0.9$ ). Further, it is quite interesting to observe the sequential changes in magneto-optical properties with in-situ microwave resonance (ESR) technique.

## Experimental

### Materials and instruments

The chemicals nickel chloride, ferric chloride ( $\text{FeCl}_3$ , Mw 162.21, 98%) and cobaltous chloride ( $\text{CoCl}_2 \cdot 6\text{H}_2\text{O}$ , Mw 291.02, 99%) from acros organics; aqueous ammonia ( $\text{NH}_3$ , Mw 17.03, 25% w/w) and ( $\text{Ni}(\text{NO}_3)_2 \cdot 6\text{H}_2\text{O}$ , Mw 290.81, 98%) were purchased from Merck; oleic acid  $\text{C}_{18}\text{H}_{34}\text{O}_2$ , Mw 282.47, 98%) was supplied by Thomas baker; deionized water from Millipore Direct Q5 (resistivity 18.2 M $\Omega$  cm).

Nanoparticles were annealed in M/s Carbolite make Muffle furnace. The structural characterization of samples was performed by Rigaku powder X-ray diffractometer with Cu-K $\alpha$  radiation, 40kVA & 30mA with step size  $0.02^\circ/\text{min}$ , scan range ( $2\theta$ ) from  $20^\circ$ - $70^\circ$ . The morphological and atomic scale image of the lattice was performed using M/s Tecnai F30 HRTEM. The specimens for HRTEM characterization were prepared by dispersing nanoparticles in heptane and then subsequently deposited on carbon-coated Cu-TEM grid (400 meshes). The film on the TEM grid was allowed to evaporate on its own. After drying, the specimen was transferred into microscope for imaging. The magnetization measurements were carried out on these samples by a search coil method. A polytronic power supply (ModelBCS-1000), electromagnet (Type Hem-100) and flux meter (Model FM109) were used for this purpose. The setup was calibrated using the standard nickel sample. The microwave spin resonance measurements were performed using X-band, 9.54 GHz, model A-300 from M/s Bruker biospin, Germany. The instrument was calibrated at room temperature using 1mg DPPH standard. To study the photomagnetic effect, the resonance spectra were irradiated first with UV radiation ( $\lambda = 200$ - $400$  nm, power = 100W) in a resonator cavity of ESR for 5 minutes in a quartz capillary. Then, after switching off lamp, the spectra were recorded as usual.

### Synthesis of $\text{Ni}_x\text{Co}_{1-x}\text{Fe}_2\text{O}_4$ nanoparticles

In the present work, we have synthesized nanoparticles by chemical coprecipitation route [33, 34] as it is relatively simpler and has potential in producing desired sized nanoparticles as compared to other methods. Furthermore, by keeping nucleation rate higher than particle growth one can obtain nanoparticles of desired shape [35]. In the

procedure of making  $\text{Ni}_x\text{Co}_{1-x}\text{Fe}_2\text{O}_4$ ;  $x=0.1$ , a homogeneous aqueous solutions of 0.1M  $\text{Ni}(\text{NO}_3)_2 \cdot 6\text{H}_2\text{O}$ , 0.9M  $\text{Co}(\text{NO}_3)_2 \cdot 6\text{H}_2\text{O}$  and 2M  $\text{FeCl}_3$  were prepared in 100mL double distilled water. Then, 2mL oleic acid was added to the mixture. Thereafter, temperature of mixture was maintained at  $80^\circ\text{C}$  ( $\pm 0.1^\circ\text{C}$ ) on constant temperature bath. The size distribution of particles, nucleation and particle growth processes were regulated via quick base addition (4M NaOH solution) with vigorous stirring by homogenizer Micra RT till pH 9 was attained. The temperature  $80^\circ\text{C}$  was maintained throughout reaction for 1 hour. After, 1 hour the obtained precipitate was dried till we get its powdered form. Then, annealing was performed in a muffle furnace at  $200^\circ\text{C}$  ( $5^\circ\text{C}/\text{min}$ ) for 2 hours. Similarly, other samples (i.e.  $x = 0.3, 0.5, 0.7, 0.9$ ) were prepared by controlling the initial stoichiometry of reactants.

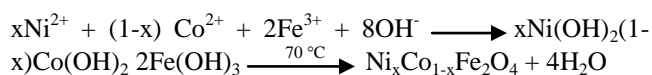
## Results and discussion

### Reaction mechanism

It is a well-known fact that all transition metal undergo hydrolysis in aqueous solutions. On similar basis, we can assume that first there was a formation of metal aquo complexes in solution.



Addition of base (NaOH) acts as a driving force for the hydrolysis for these aquo complexes resulting in their hydroxides. Heating at  $80^\circ\text{C}$  for 1 hour transforms the precipitate into  $\text{Ni}_x\text{Co}_{1-x}\text{Fe}_2\text{O}_4$  nanocrystallites. Keeping in mind the above possibilities, the overall reaction can be summarized as:



To control the size distribution of  $\text{Ni}_x\text{Co}_{1-x}\text{Fe}_2\text{O}_4$  particles, nucleation and particle growth process were regulated via quick base addition with vigorous stirring. This was done in light of LaMer method for obtaining monodisperse particles [35]. The obtained precipitate was washed several times with hexane-acetone-water mixture (1:3:1). To further narrow down the size distribution, the product was centrifuged at 10000 rpm for 5 min. Finally, obtained nanoparticles were then dried in air at  $60^\circ\text{C}$  for 4 hours.

### Structural characterization

X-ray diffraction pattern of as prepared  $\text{Ni}_{0.5}\text{Co}_{0.5}\text{Fe}_2\text{O}_4$  is shown in **Fig. 1(a)**. The broad diffraction peaks were due to weakly crystallized phase of metal-oxyhydroxide. This resembles the ferrihydrite phase prior to the formation of  $\text{Fe}_3\text{O}_4$ . To improve the crystallinity, the samples were annealed at  $200^\circ\text{C}$  in air for 2 hours and their respective XRD patterns are shown in (**Fig. 1(b) - (f)**) which indicates two well-reported transformations.

Firstly, there was a structural transformation of nanoparticles, i.e. improvement in size as well as crystallinity of ferrimagnetic core and decrease in thickness of outer amorphous shell as shown in **Fig. 2**. Secondly, the

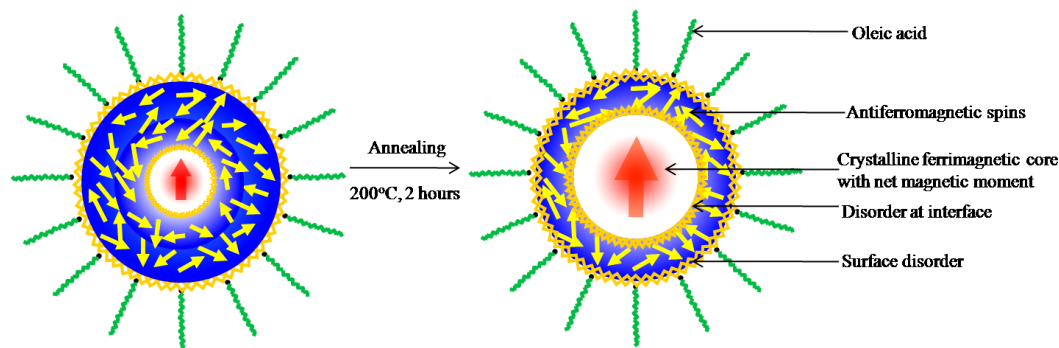


Fig. 2 Structural transformations in the nanoparticles due to annealing.

peak shift and lower intensity of diffraction pattern indicate the defect due to nanocrystalline forms [23-26, 35, 36]. The phase identification confirms the single phase of cubic spinel structure (JCPDS 00-022-1086 and 00-010-0325). This is in contrast with Maaz et al. [37]. It may be due to the fact that our annealing temperature was well below 600°C (i.e. 200°C).

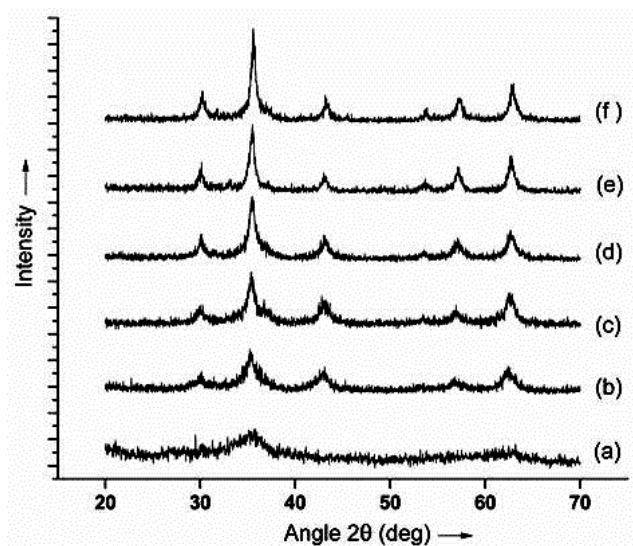


Fig. 1. XRD pattern of (a) as synthesized  $\text{Ni}_{0.5}\text{Co}_{0.5}\text{Fe}_2\text{O}_4$  and annealed samples (b-f) at 200°C, (b)  $\text{Ni}_{0.1}\text{Co}_{0.9}\text{Fe}_2\text{O}_4$ , (c)  $\text{Ni}_{0.3}\text{Co}_{0.7}\text{Fe}_2\text{O}_4$ , (d)  $\text{Ni}_{0.5}\text{Co}_{0.5}\text{Fe}_2\text{O}_4$ , (e)  $\text{Ni}_{0.7}\text{Co}_{0.3}\text{Fe}_2\text{O}_4$ , (f)  $\text{Ni}_{0.9}\text{Co}_{0.1}\text{Fe}_2\text{O}_4$ .

The average crystallite size and strain induced in this polycrystalline material was calculated from Williamson-Hall method;  $\beta \cos\theta = 4\epsilon \sin\theta + \lambda/D$  where,  $D$  is the crystallite size,  $\lambda$  is the wavelength of the X-ray,  $\beta$  is full width at half maximum (FWHM) measured in radians,  $\epsilon$  is the induced strain in system, and  $\theta$  is the Bragg angle. Various structural parameters derived from XRD patterns are given in Table 1. It was seen that average crystallite size varies between 13.6 to 5.1 nm with the increase of  $\text{Co}^{2+}$  concentration from 0.1 to 0.9. The lattice parameter, 'a' was found to increase with  $\text{Co}^{2+}$  concentration due to bigger ionic radii of  $\text{Co}^{2+}$  over  $\text{Ni}^{2+}$ . The decrease in  $\langle D \rangle$  value with increase in  $\text{Co}^{2+}$  was attributed to the defect introduced in the lattice structure by larger  $\text{Co}^{2+}$  ions. Further, the

strain relieves surface to volume ratio as the crystallite size gradually increased (Table 1).

Table 1. Structural parameters calculated from XRD patterns.

Composition	Crystallite size $D$ (nm)	(a) (Å)	Strain
$\text{Ni}_{0.1}\text{Co}_{0.9}\text{Fe}_2\text{O}_4$	5.1	8.3824	-0.0105
$\text{Ni}_{0.3}\text{Co}_{0.7}\text{Fe}_2\text{O}_4$	7.9	8.3723	-0.0075
$\text{Ni}_{0.5}\text{Co}_{0.5}\text{Fe}_2\text{O}_4$	9.2	8.3682	-0.0053
$\text{Ni}_{0.7}\text{Co}_{0.3}\text{Fe}_2\text{O}_4$	12.8	8.3566	-0.0028
$\text{Ni}_{0.9}\text{Co}_{0.1}\text{Fe}_2\text{O}_4$	13.6	8.3448	-0.0015

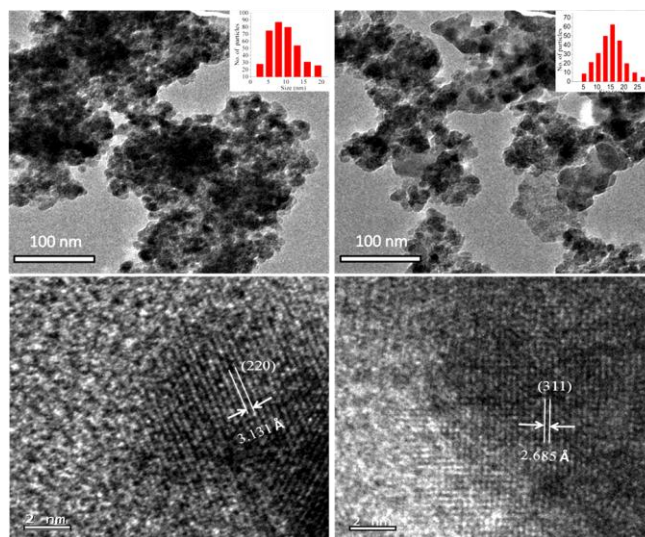


Fig. 3. TEM images of (a)  $\text{Ni}_{0.1}\text{Co}_{0.9}\text{Fe}_2\text{O}_4$  and (b)  $\text{Ni}_{0.9}\text{Co}_{0.1}\text{Fe}_2\text{O}_4$  nanoparticles with inset showing particle size distribution. (c) and (d) shows HRTEM images with indexed interplanar spacings (d-value).

Transmission electron microscope images of  $\text{Ni}_{0.1}\text{Co}_{0.9}\text{Fe}_2\text{O}_4$  and  $\text{Ni}_{0.9}\text{Co}_{0.1}\text{Fe}_2\text{O}_4$  samples are shown in Fig. 3 (a) and (b) respectively. The average particle sizes obtained from the images were  $\sim 7.8$  nm and  $\sim 16.2$  nm and almost all particles are spherical in shape. The inset shows the size distribution of particles. These results are in well agreement with XRD data, however the difference in observed sizes was due to the existence of amorphous surface layer around the individual nanoparticles. The respective high resolution TEM images are shown in Fig. 3 (c), (d). The measured interplanar spacing 'd' values

were systematically slightly larger than the standard values of which corroborates the fact that the strain has been induced in the samples.

### Magnetic characterization

**Fig. 4** shows magnetization measurement of the samples at room temperature. All the samples were found to be in the superparamagnetic regime as they shown zero remanance and zero coercivity (**Fig. 4(a)**). To describe the magnetization of these systems, we used Langevin function:

$$M(T) = M_s L(x) = M_s \left[ \coth(x) - \frac{1}{x} \right]$$

$$= M_s \left( \frac{e^x + e^{-x}}{e^x - e^{-x}} - \frac{1}{x} \right) ; x = \frac{\mu H}{k_B T}$$

where  $M(T)$  is the magnetization of samples at temperature  $T$ ,  $M_s$  represents the saturation magnetization of nanomaterial,  $\mu$  is the magnetic moment of particles ( $\mu = M_{s(\text{bulk})} V$ ) and  $V$  is the volume of particles. The reported  $M_{s(\text{bulk})}$  values of  $\text{NiFe}_2\text{O}_4$  and  $\text{CoFe}_2\text{O}_4$  are 50 and 80 emu/g [38]. Assuming the linear behavior of bulk magnetization across stoichiometric variation of  $\text{Co}^{2+}$  and  $\text{Ni}^{2+}$  in  $\text{M}^{2+}\text{Fe}^{3+}_2\text{O}_4$ , the calculated  $M_{s(\text{bulk})}$  values are 77, 71, 65, 59 and 53 emu/g (**inset Fig. 4(a)**). These values were further used for curve fitting as shown in **Fig 4(b)**.

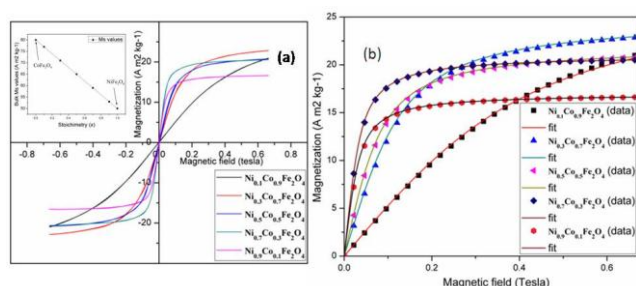


**Fig. 4.** (a) Magnetization measurement of  $\text{Ni}_x\text{Co}_{1-x}\text{Fe}_2\text{O}_4$  ( $x=0.1-0.9$ ) annealed at  $200^\circ\text{C}$ . The inset shows the bulk magnetization values of  $\text{Ni}_x\text{Co}_{1-x}\text{Fe}_2\text{O}_4$  ( $x = 0, 0.1, 0.3, 0.5, 0.7, 0.9, 1$ ). (b) The fitted Langevin function curves for  $\text{Ni}_x\text{Co}_{1-x}\text{Fe}_2\text{O}_4$ .

The derived parameters;  $M_s$  and  $D_m$  (magnetic size of particles) obtained from the fitting procedure are listed in **Table 2**. The magnetic size of particles  $D_m$ , thus calculated was consistently smaller than those observed in XRD and TEM measurement. Also,  $M_s$  values were lesser than their corresponding  $M_{s(\text{bulk})}$  values. Both these observations are well reported in the literature and can be ascribed to core-shell structure, spin canting phenomena, spin-glass, surface spin disorder and frustration of AFM exchange interactions [39-43]. Further,  $M_s$  values are found to decrease with increasing  $\text{Ni}^{2+}$  content. The reason is, as more and more  $\text{Ni}^{2+}$  was introduced in the lattice, there was replacement of  $\text{Fe}^{3+}$  by  $\text{Ni}^{2+}$  ions on the octahedral sites; as  $\text{Ni}^{2+}$  has greater octahedral site preference energy [44, 45].

The X-band ESR experiment was performed to understand superexchange, dipolar interactions, core-shell structure and their consequential role in observing photomagnetic effect on UV irradiation. The measurement has been performed on 1mg of each samples in two sets; 1)

The resonance spectra were recorded without UV irradiation, 2) samples were irradiated with UV for 5 minutes.

**Table 2.** Value of fitted parameters obtained from Langevin function for different compositions.

Composition	Magnetic size $D$ (nm)	$M_s$ (emu/g)
$\text{Ni}_{0.1}\text{Co}_{0.9}\text{Fe}_2\text{O}_4$	4.9	28.2
$\text{Ni}_{0.3}\text{Co}_{0.7}\text{Fe}_2\text{O}_4$	7.3	25.3
$\text{Ni}_{0.5}\text{Co}_{0.5}\text{Fe}_2\text{O}_4$	8.7	22.1
$\text{Ni}_{0.7}\text{Co}_{0.3}\text{Fe}_2\text{O}_4$	11.9	21.7
$\text{Ni}_{0.9}\text{Co}_{0.1}\text{Fe}_2\text{O}_4$	12.5	17.4

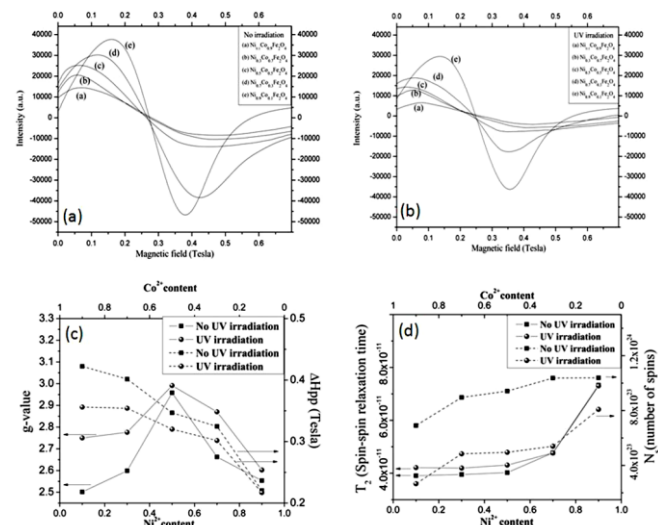


**Fig. 5.** (a) and (b) shows the microwave resonance spectra of with and without UV irradiation respectively. The parameters derived from the spectra; g-value, peak-to-peak linewidth ( $\Delta H_{pp}$ ), spin-spin relaxation time ( $T_2$ ) and numbers of spins ( $N_s$ ) are shown in (c) and (d).

### ESR measurement

Based on structural and magnetic measurement findings we suggest a surfacted core-shell model, where the core is ferromagnetic (FM) in nature and shell is antiferromagnetic (AFM) in nature. The outer AFM surface layer is expected to behave like a spin glass layer which in turn is coated by surfactant. So, the extent of superexchange in core was expected to be more as compared to that in shell [26, 46]. Without UV irradiation, a non-monotonous behavior for resonance field with different composition was observed. Initially, g-value increases from  $x = 0.1 - 0.5$  and later decreases for  $x = 0.5 - 0.9$ . This was attributed to the effectiveness of superexchange via same cations  $\text{Ni}^{2+} - \text{O} - \text{Ni}^{2+}$  or  $\text{Co}^{2+} - \text{O} - \text{Co}^{2+}$  in core, over the case where different cations were available for superexchange i.e.  $\text{Co}^{2+} - \text{O} - \text{Ni}^{2+}$  [47]. Here, obviously the contribution of superexchange from FM core was expected to be more than outer AFM layer (**Fig. 1**). However, spectra broadening were observed in all the samples. It may be due to spread of resonance fields for randomly oriented nanoparticles (anisotropy broadening). It was seen that the peak to peak linewidth ( $\Delta H_{pp}$ ) increased with  $\text{Co}^{2+}$  content which was attributed to the larger magnetocrystalline anisotropy of

Co<sup>2+</sup>, which in turn enhanced the dipolar interactions among nanoparticles [48]. The spin-spin relaxation time (T<sub>2</sub>) was calculated by following equation:

$$T_2 = \frac{\hbar}{\sqrt{3} \Delta H_{pp} g \beta}$$

The calculated T<sub>2</sub> values have been found to decrease with increase in Co<sup>2+</sup> content. It may be due to the hindrance in relaxation of resonated nanoparticles, as the dipolar interaction increases with Co<sup>2+</sup> in the system. Numbers of spins (N<sub>s</sub>) in the samples were calculated by comparing the intensity of absorption curves with that of 1mg standard DPPH sample. It was found that N<sub>s</sub> decreases consistently as Co<sup>2+</sup> content increases. This has been correlated to the relative magnitudes of magnetic moments of Co<sup>2+</sup> and Ni<sup>2+</sup> as explained in section 3.3.

In another set of resonance experiment, the room temperature spectra of all the samples with UV irradiation show a remarkable change in their magneto-optical properties. After irradiation, g-value increases for all the samples while maintaining their nonmonotonous behavior. Invoking the principle of surface-volume effect in nanoparticles, we simply assumed that surface of nanoparticles was mainly affected by UV irradiation. As a result, electronic transitions mainly involved at surface atoms of the particles were responsible for further decrease in extent of superexchange in outer shell. Hence, increased g values after irradiation were expected on this basis. Decrease in ΔH<sub>pp</sub> values after irradiation was explained as the decrease in dipolar interactions. This is due to the fact that this interaction has the tendency to inhibit the easy alignment of nanoparticles along the applied field direction. So, after reduced core-shell interaction due to electronic transitions, shell along with outer structure would be acting more as a magnetically non interacting matrix. As a result, particles would be aligning more swiftly with sweeping magnetic field. This reasoning is similar to the fact that in presence of dipolar interactions, coercivity reduces for a noninteracting assembly [49]. Concomitantly, reduced dipolar interactions (due to non-interacting matrix behavior) were also responsible for decreasing ΔH<sub>pp</sub> values. Spin-spin relaxation time (T<sub>2</sub>) increases for all the stoichiometries after irradiation. This can also be explained on the same basis that spin-spin relaxation of nanoparticles will now be on individual basis due to non-interacting assembly behavior. Alongside, N<sub>s</sub> has been found to be decreased after irradiation because of electronic transitions taking place at surface atoms as well as probable electron transfer between Co<sup>2+</sup> and Fe<sup>3+</sup>. Therefore, lesser number of electrons would have been available for microwave assisted transitions.

## Conclusion

Nanocrystalline Ni<sub>x</sub>Co<sub>1-x</sub>Fe<sub>2</sub>O<sub>4</sub> (0.1≤x≤0.9) has been synthesized. Mutual stoichiometric variation of Ni<sup>2+</sup> and Co<sup>2+</sup> in the system showed systematic changes in structural properties like, lattice parameter, crystallite size, and particle size distribution. Both structural and magnetic parameters have been correlated to understand the core

shell structure by superexchange, dipolar interactions and electronic transitions. To the best of our knowledge, this is the first report of UV induced changes in photomagnetic properties of this material. Further investigations are needed to be explored this behavior in detail to achieve potential application of the material.

## Acknowledgement

The authors are thankful to Director, National Physical Laboratory for his support and continuous encouragement for carrying out the research work.

## Reference

- Hersam, M. *ACS Nano*, **2011**, 5, 1.  
DOI: [10.1021/nn103470j](https://doi.org/10.1021/nn103470j).
- Tiwari, A., *Advanced Materials Letters*, **2012**, 3, 172.  
DOI: [10.5185/amlett.2012.2002](https://doi.org/10.5185/amlett.2012.2002).
- Kamat, P.V.; Meisel, D. *C. R. Chimie*, **2003**, 6, 1999.  
DOI: [10.1016/j.crci.2003.06.005](https://doi.org/10.1016/j.crci.2003.06.005).
- Odom, T.W.; Pileni, M.P., *Accounts of chemical research* **2008**, 41, 1565.  
DOI: [10.1021/ar800253n](https://doi.org/10.1021/ar800253n).
- Murray R.W., *Analytical Chemistry* **2001**, 73, 645 A.  
DOI: [10.1021/ac012641y](https://doi.org/10.1021/ac012641y).
- Bader, S.D., *Reviews of modern physics*, **2006**, 78, 1.  
DOI: [10.1103/RevModPhys.78.1](https://doi.org/10.1103/RevModPhys.78.1).
- Hiergeist, R.; Andrä, W.; Buske, N.; Hergt, R.; Hilger, I.; Richter, U.; Kaiser, W. *Journal of Magnetism and Magnetic Materials* **1999**, 201, 420.  
DOI: [10.1016/S0304-8853\(99\)00145-6](https://doi.org/10.1016/S0304-8853(99)00145-6).
- Mee, C.D.; Daniel, E.D. *Magnetic Recording Technology*, 2nd edn, McGraw Hill, New York **1996**.
- McMichael, R.D.; Shull R.D.; Swartzendruber L.J.; Bennett L.H.; Watson R.E. *Journal of magnetism and magnetic materials* **1992**, 111, 29.  
DOI: [10.1016/0304-8853\(92\)91049-Y](https://doi.org/10.1016/0304-8853(92)91049-Y).
- Gschneidner, K.A.; Pecharsky, V.K. *Journal of Applied Physics* **1999**, 85, 5365.  
DOI: [10.1063/1.369979](https://doi.org/10.1063/1.369979).
- Sankar, S.; Dender, D.; Borchers, J.A.; Smith, D.J.; Erwin, R.W.; Kline, S.R.; Berkowitz, A.E. *Journal of magnetism and magnetic materials* **2000**, 221, 1.  
DOI: [10.1016/S0304-8853\(00\)00391-7](https://doi.org/10.1016/S0304-8853(00)00391-7).
- Baruwati B.; Nadagouda, M.N.; Varma R.S. *Journal of Physical Chemistry C* **2008**, 112, 18399.  
DOI: [10.1021/jp807245g](https://doi.org/10.1021/jp807245g).
- Shafi, K.V.P.M.; Koltypin, Y.; Gedanken, A. *Journal of Physical Chemistry B* **1997**, 101, 6409.  
DOI: [10.1021/jp970893q](https://doi.org/10.1021/jp970893q).
- Yan, A.; Liu, X.; Yi R.; Shi, R.; Zhang, N.; Qiu, G. *Journal of Physical Chemistry C* **2008**, 112, 8558.  
DOI: [10.1021/jp800997z](https://doi.org/10.1021/jp800997z).
- Kulthe M.G.; Goyal, R.K., *Advanced Materials Letters* **2012**, 3, 246.  
DOI: [10.5185/amlett.2012.3326](https://doi.org/10.5185/amlett.2012.3326).
- Singh, M.; Kumar, M.; Štěpánek, F.; Ulbrich, P.; Svoboda, P.; Santava, E.; Singla, M.L., *Advanced Materials Letters* **2011**, 2, 409.  
DOI: [10.5185/amlett.2011.4257](https://doi.org/10.5185/amlett.2011.4257).
- Prakash, J.; Tripathi, A.; Pivin, J.C.; Tripathi, J.; Chawla, A.K.; Chandra, R.; Kim, S.S.; Asokan, K.; Avasthi, D.K., *Advanced Materials Letters* **2011**, 2, 71.  
DOI: [10.5185/amlett.2010.12187](https://doi.org/10.5185/amlett.2010.12187).
- Li, Y.; Fang, Q.; Liu, Y.; Lv, Q.; Yin, P. *Journal of Magnetism and Magnetic Materials* **2007**, 313, 57.  
DOI: [10.1016/j.jmmm.2006.12.003](https://doi.org/10.1016/j.jmmm.2006.12.003).
- Ayyappan, S.; Mahadevan, S.; Chandramohan, P.; Srinivasan, M.P.; Philip, J.; Raj, J. *Journal of Physical Chemistry C* **2010**, 114, 6334.  
DOI: [10.1021/jp911966p](https://doi.org/10.1021/jp911966p).
- Giri, A.K.; Pellerin, K.; Pongsaksawad, W.; Sorescu, M.; Majetich, S.A. *IEEE Transactions in Magnetism* **2000**, 36, 3029.  
DOI: [10.1109/20.908666](https://doi.org/10.1109/20.908666).

21. Giri, A.K.; Kirkpatrick, E.M.; Moongkhamklang, P.; Majetich, S.A.; Harris, V.G. *Applied Physics Letters* **2002**, 80, 2341.  
DOI: [10.1063/1.1464661](https://doi.org/10.1063/1.1464661).
22. Kawamoto, T.; Asai, Y.; Abe, S. *Physical Review Letters* **2001**, 86, 348-351.  
DOI: [10.1103/PhysRevLett.86.348](https://doi.org/10.1103/PhysRevLett.86.348).
23. Kumar, V.; Rana, A.; Yadav, M.S.; Pant, R.P. *Journal of Magnetism and Magnetic Materials* **2008**, 320, 1729.  
DOI: [10.1016/j.jmmm.2008.01.021](https://doi.org/10.1016/j.jmmm.2008.01.021).
24. Vestal, C.R.; Zhang, Z.J. *Nano Letters*. **2003**, 3, 1739.  
DOI: [10.1021/nl034816k](https://doi.org/10.1021/nl034816k).
25. Dai, Q.; Lam, M.; Swanson, S.; Yu, R.R.; Milliron, D.J.; Topuria, T.; Jubert, P.; Nelson, A. *Langmuir* **2010**, 26, 17546.  
DOI: [10.1021/la103042q](https://doi.org/10.1021/la103042q).
26. Kodama, R.H.; Berkowitz, A.E. *Physical Review Letters* **1996**, 77, 394.  
DOI: [10.1103/PhysRevLett.77.394](https://doi.org/10.1103/PhysRevLett.77.394).
27. Singhal, S.; Singh, J.; Barthwal, S.K.; Chandra, K.; *Journal of Solid State Chemistry* **2005**, 178, 3183.  
DOI: [10.1016/j.jssc.2005.07.020](https://doi.org/10.1016/j.jssc.2005.07.020).
28. Gul, I.H.; Amina, F.; Abbasi, A.Z.; Anis-ur-Rehman, M.; Maqsood, A. *Scripta materialia* **2007**, 56, 497.  
DOI: [10.1016/j.scriptamat.2006.11.020](https://doi.org/10.1016/j.scriptamat.2006.11.020).
29. Dixit, G.; Singh, J.P.; Srivastava, R.C.; Agrawal, H.M.; Chaudhary, R.J.; *Advanced Materials Letters* **2012**, 3, 21.  
DOI: [10.5185/amlett.2011.6280](https://doi.org/10.5185/amlett.2011.6280).
30. Upadhyay, R.V.; Parekh, K.; Mehta, R.V. *Physical Review B* **2003**, 68, 224434-1.  
DOI: [10.1103/PhysRevB.68.224434](https://doi.org/10.1103/PhysRevB.68.224434).
31. Webb, D.J.; Bhagat, S.M. *Journal of Magnetism Magnetic Materials* **1984**, 42, 109.  
DOI: [10.1016/0304-8853\(84\)90298-1](https://doi.org/10.1016/0304-8853(84)90298-1).
32. Webb, D.J.; Bhagat, S.M. *Journal of Magnetism Magnetic Materials* **1984**, 42, 121.  
DOI: [10.1016/0304-8853\(84\)90299-3](https://doi.org/10.1016/0304-8853(84)90299-3).
33. Rabias, I.; Fardis, M.; Devlin, E.; Boukos, N.; Tsiroli, D.; Papavassiliou, G., *Acs nano* **2008**, 2, 977.  
DOI: [10.1021/nn700414w](https://doi.org/10.1021/nn700414w).
34. Kim, Y.; Kim, D.; Lee, C.S., *Physica B: Condensed Matter* **2003**, 337, 42.  
DOI: [10.1016/S0921-4526\(03\)00322-3](https://doi.org/10.1016/S0921-4526(03)00322-3).
35. LaMer, V.K.; Dinegar, R.H. *Journal of American Chemical Society* **1950**, 72, 4847.  
DOI: [10.1021/ja01167a001](https://doi.org/10.1021/ja01167a001).
36. Schmid, G.; Nanoparticles: Magnetic Nanoparticles', 2nd edn, **2011**, Germany Wiley-VCH Verlag GmbH & Co.
37. Maaz, K.; Karim, S.; Mashiatullah, A.; Liu, J.; Hou, M.D.; Sun, Y.M.; Duan, J.L.; Yao, H.J.; Mo, D.; Chen, Y. *Physica B: Condensed Matter* **2009**, 404, 3947.  
DOI: [10.1016/j.physb.2009.07.134](https://doi.org/10.1016/j.physb.2009.07.134).
38. Cullity, B.D. Introduction to magnetic materials', 2nd edn, **2009**, New Jersey Wiley.
39. Hergt, R.; Hiergeist, R.; Zeisberger, M.; Glöckl, G.; Weitschies, W.; Ramirez, L.P.; Hilger, I.; Kaiser, W.A. *Journal of Magnetism and Magnetic Materials* **2004**, 280, 358.  
DOI: [10.1016/j.jmmm.2004.03.034](https://doi.org/10.1016/j.jmmm.2004.03.034).
40. Kommareddi, N.S.; Tata, M.; John, V.T.; McPherson, G.L.; Herman, M.F.; Lee, Y.S.; O'Connor, C.J.; Akkara, J.A.; Kaplan, D.L.; *Chemistry of Materials* **1996**, 8, 801.  
DOI: [10.1021/cm940485o](https://doi.org/10.1021/cm940485o).
41. Tung, L.D.; Kolesnichenko, V.; Caruntu, D.; Chou, N.H.; O'Connor, C.J. *Journal of Applied Physics* **2003**, 93, 7486.  
DOI: [10.1063/1.1540145](https://doi.org/10.1063/1.1540145).
42. Grigorova, M.; Blythe, H.J.; Blaskov, V.; Rusanov, V.; Petkov, V.; Masheva, V.; Nihtianova, D.; Martinez, L.M.; Muñoz, J.S.; Mikhov, M. *Journal of magnetism and magnetic materials* **1998**, 183, 163.  
DOI: [10.1016/S0304-8853\(97\)01031-7](https://doi.org/10.1016/S0304-8853(97)01031-7).
43. Shafi, K.V.P.M.; Gedanken, A.; Prozorov, R.; Balogh, J.; *Chemistry of Materials* **1998**, 10, 3445.  
DOI: [10.1021/cm980182k](https://doi.org/10.1021/cm980182k).
44. McClure, D.S. *Journal of Physics and Chemistry of Solids* **1957**, 3, 311.  
DOI: [10.1016/0022-3697\(57\)90034-3](https://doi.org/10.1016/0022-3697(57)90034-3).
45. Grimes, R.W.; Anderson, D.S.; Heuer, A.H. *Journal of American Chemical Society* **1989**, 111, 1-7.  
DOI: [10.1021/ja00183a001](https://doi.org/10.1021/ja00183a001).
46. Kodama, R.H.; Berkowitz, A.E.; *Physical Review B* **1999**, 59, 6321.  
DOI: [10.1103/PhysRevB.59.6321](https://doi.org/10.1103/PhysRevB.59.6321).
47. Shahane, G.S.; Kumar, A.; Arora, M.; Pant, R.P.; Lal, K. *Journal of Magnetism and Magnetic Materials* **2010**, 322, 1015.  
DOI: [10.1016/j.jmmm.2009.12.006](https://doi.org/10.1016/j.jmmm.2009.12.006).
48. Gubin, S.P.; Magnetic nanoparticles, 1st edn, **2009**, Weinheim Wiley-VCH Verlag GmbH & Co.
49. Kechrakos, D.; Trohidou, K.N.; *Physical Review B* **1998**, 58, 12169.  
DOI: [10.1103/PhysRevB.58.12169](https://doi.org/10.1103/PhysRevB.58.12169).

**Advanced Materials Letters**

Publish your article in this journal

ADVANCED MATERIALS Letters is an international journal published quarterly. The journal is intended to provide top-quality peer-reviewed research papers in the fascinating field of materials science particularly in the area of structure, synthesis and processing, characterization, advanced-state properties, and applications of materials. All articles are indexed on various databases including DOI and are available for download for free. The manuscript management system is completely electronic and has fast and fair peer-review process. The journal includes review articles, research articles, notes, letter to editor and short communications.

